University of Bath

Alternative formats
If you require this document in an alternative format, please contact:
openaccess@bath.ac.uk

Viscoelastic embedment behaviour of dowels and screws under in-service vibration

Thomas Reynolds (corresponding author)
Richard Harris
Wen-Shao Chang

BRE Centre for Innovative Construction Materials
University of Bath, Claverton Down, Bath BA2 7AY UK
Tel.: +44(0)1225385943
Fax: +44(0)1225386691
tpsr20@bath.ac.uk

Abstract

Dowel and screw connections in timber structures behave nonlinearly, even at loads which would be experienced in a structure in normal service. They exhibit hysteresis and creep as a result of both the viscoelastic behaviour of the timber itself and the frictional interaction between the timber and connecting elements, and stress concentrations are created which behave plastically, even at loads well below the nominal yield force of the connection. A fundamental process in the load transfer through such a connection is the embedment of the connector into the timber that surrounds it, and the frictional, nonlinear and time-dependent properties in that process are investigated here. A simple rheological model, a combination of Kelvin-Voigt viscoelastic elements, was fitted to the measured response of a block of timber in embedment by a plain dowel or screw. Experiments were performed in which an oscillating force was applied to the screw or dowel, representative of in-service vibration in a timber structure. The effects of plasticity and viscoelasticity were quantified by comparing equivalent linear stiffnesses for an oscillating load, a short-term change in static load, and an initial static loading. The results showed a stiffness, on average, 3.8 times higher under oscillating load than under initial static loading with the same peak force. By quantifying and modelling viscoelastic behaviour in timber around a connector, this work contributes to the development of damping and stiffness models for joints under oscillating load. Such models could be used to determine the contribution of connections to the dynamic response of long spans and tall buildings in timber.

Keywords

viscoelastic; vibration; foundation modulus; dowel; screw; serviceability; connection; stiffness

1 Introduction

Dowel-type connections are widely used. They include bolts, screws, nails and plain dowels. One of the fundamental components of the load transfer in a dowel-type

connection is the embedment of the connector into the timber which surrounds it. The work presented in this study examines the deformation and energy dissipation of timber in embedment by a dowel or screw under loads representative of in-service vibration. It evaluates, through experiment and fitting of a rheological model, the time-dependency and energy dissipation of the timber in embedment by a connector.

The time-history of force applied to the timber was chosen to be representative of in-service vibration of structures, consisting of a mean force plus an oscillating component. This corresponds to, for example, the mean load from the self-weight and imposed load of a bridge or floor structure plus a dynamic load imposed by footfall, or the steady component of a wind force plus an oscillating component from turbulence. The peak values of the force were chosen to reflect the magnitude of the forces regularly experienced by a structure in service due to normal loading.

The behaviour of timber in embedment by a connector is not linear-elastic. The timber itself behaves in a viscoelastic way, giving time-dependent creep or stress relaxation, even in the timescale considered in this work. Friction between the face of the dowel and the timber also contributes to the force transfer, and dissipates energy under cycles of load. Furthermore, the imperfection of the contact face between dowel and timber means that some initial deformation of the joint is required to achieve full contact, meaning that the joint does not exhibit its full stiffness under small deformations. Finally, stress concentrations due to inaccuracies in construction and unevenness in the contact surfaces can result in regions of plasticity in the timber, even under loads below the embedment strength.

If an elastic analysis is to be carried out for a timber structure with such connections it must, therefore, use an approximation of the joint stiffness appropriate to a particular applied force. As a result, the stiffness used to calculate the overall deflection due to a long-term static load must be different to that used for the relative deflection under a short-term, small-amplitude oscillating force, such as might be experienced by a structure vibrating due to wind or footfall. This work seeks to quantify the components of the deflection of a dowel-type connector by fitting a simple rheological model to the response, which allows for viscoelasticity and local plastic behaviour.

In analysis of connections, the stiffness of the timber in embedment by the dowel is described by the foundation modulus, which represents the interaction between the steel dowel and the timber which surrounds it. The behaviour of a particular connection is then predicted using the foundation modulus in conjunction with the geometry of the connection and the properties of the connectors.

The analysis and experimental work described here produces a foundation model for the timber in embedment. Using this model, the response can be divided into viscoelastic and plastic components, which have been quantified and used to compare the different timbers and connectors which have been tested. This foundation model could then be used to predict the behaviour of complete connections under in-service loads and vibration.

2 Background

2.1 Stiffness models

In Eurocode 5 (BSI 2009), the deformation of dowel-type connections is determined using the parameter K_{ser}, which was defined by fitting an empirical model to connection test data, in work reported by Ehlbeck and Larsen (1991).

More recently, researchers have presented models for the stiffness of connections under dynamic loads (Chui and Li, 2005; Awaludin et al, 2007, 2008a; Foschi, 2000) based on the material properties of the dowel and the foundation modulus of the timber. The foundation modulus represents the embedment behaviour of the timber around the dowel, and is obtained from tests (Foschi et al, 2000; Chui and Ni, 1997). These models analyse the interaction of dowel and timber, and so take into account the geometry of a particular connection, and can be applied to a wider range of connections than a purely empirical model. They rely on the foundation modulus obtained from tests, and the tests which have been carried out have been generally representative of seismic loading on structures. The study presented here investigates the foundation modulus for in-service loading.

2.2 Viscoelasticity

Researchers have modelled the time-dependent behaviour of timber components, for periods from hours to years, by viscoelastic models (Jiali and Jianxiong, 2009; Schniewind and Barrett, 1972; Sun et al, 2007). Rheological models consisting of generalizations of the Kelvin-Voigt or Maxwell mechanical models, or combinations of the two, have been proposed and tested for description of creep in timber elements (Hering and Niemz, 2012; Dinwoodie, 2000; Awaludin et al, 2008b; Lagana, 2008). The Burgers body (Burgers 1939), shown in Fig. 1 consists of a series combination of: a spring, to represent the instantaneous, linear-elastic component of the response; a spring and damper in parallel, to represent the delayed-elastic or recoverable creep component of the response; and a damper to represent the plastic or irrecoverable creep.
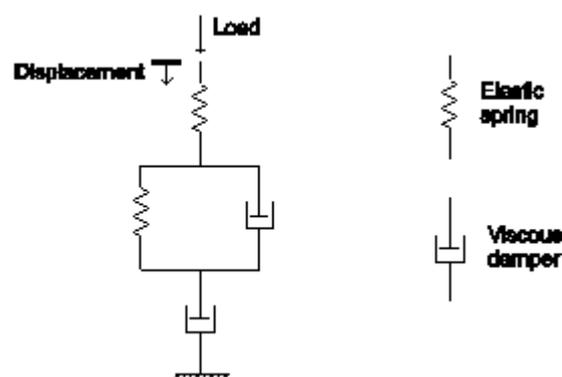
Fig. 1 Burgers body (Burgers 1939)

A Kelvin-Voigt model is applied to longitudinal creep in beech by Hering and Niemz (2012). They also recognize the independent contribution to creep caused by moisture content variations, and include an additional term to account for that effect. They use a series combination of six Kelvin-Voigt components to represent the behaviour of the material in bending under constant load over a period of 200 hours.

Generalized Kelvin-Voigt and Maxwell mechanical models, hereafter called linear rheological models, can be expressed as combinations of linear elastic springs and viscous dampers. This is not the only approach which has been used to model creep in timber. Gressel (1984) investigates four models for creep under constant load, two of which are linear rheological models based on the Burgers body, and two which raise time to a power to give displacement. The latter two cannot be readily adapted to model displacement under a time varying load, however, as required by this work.

This work extends this field by studying the short-term viscoelastic behaviour of connections, including their vibration response. A linear rheological model is applied to represent creep and hysteresis in a connection under short-term oscillating loads with a frequency of 1 Hertz and a duration of 1000 seconds. Where previous work has focussed on the fully reversed cyclic loading appropriate to seismic design, this research considers the smaller-amplitude one-sided vibration appropriate to in-service loading.

3 Method

3.1 Experimental method

3.1.1 Test setup

The tests are based on an American Society for Testing and Methods (ASTM) static test method for determination of the static embedment strength of timber under dowel-bearing (ASTM D5764). The timber specimen has a half-hole in the surface, into which a steel dowel is placed. Screw specimens are made following guidance in ASTM D5764: the timber is cut to form two specimens, which are clamped together so that the hole can be predrilled and the screw inserted into the join between the specimens.

A vertical load is then applied to the dowel or screw, and the deformation of the loading head is measured. The test setup is shown schematically in Fig. 2.
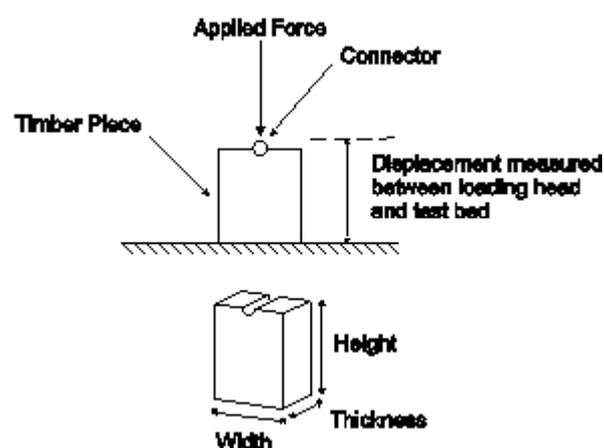

Fig. 2 Test principle and dimensions for dowel bearing test

In a real connection, the dowel passes through a complete hole in the timber, and the method used in this study therefore neglects the contribution of the timber on the unloaded side of the hole. Tests according to the European Norm for determination of

foundation modulus (EN 383) use a dowel through a complete hole in the timber. In that method, however, it is not possible to hold the dowel rigidly straight, and so the foundation modulus can only be obtained by correcting for the assumed deformation of the dowel. Given the high stiffness of the timber under oscillating load, the deformation of the dowel would represent an unacceptably high proportion of the total measured deformation, and uncertainty in the deformed shape of the dowel would make the foundation modulus unreliable.

Santos et al (2010) compared ASTM D5764 and EN 383, and, after testing 24 specimens according to each standard, found the stiffness according to the ASTM method 7.6% higher in the longitudinal grain direction and 1.2% lower in the radial direction, using no correction for dowel deformation. Given the coefficient of variation of 0.22 in the tests, these variations are small in comparison to the natural variation in the material. The ASTM method using a dowel through a half hole is, therefore, assumed to give a sufficiently accurate estimate of the foundation modulus for a dowel through a complete hole, and was used in this study to eliminate the effect of deformation of the connector.

Three different connectors were used: a 20mm diameter plain dowel; a 12mm diameter plain dowel and a continuously threaded screw with inner diameter 7.5mm and outer thread diameter 12mm. The screw specimens were predrilled to 6mm. The type of timber, grain orientation and dimensions are given in Table 1. The dimensions are chosen according to the ASTM method(ASTM D5764) and, for the sake of comparison with other work, meet the equivalent requirements in the EN method (EN 383).

Table 1 Timber species, grain orientation and dimensions

Specimen	Orientation	Height (mm)	Width (mm)	Thickness (mm)
Douglas fir and 20mm dowel	Parallel	140	120	60
	Perpendicular	80	280	60
Norway spruce and 12mm dowel	Parallel	84	72	40
	Perpendicular	50	168	40
Norway spruce and screw	Parallel	84	72	40
	Perpendicular	50	168	40

3.1.2 Estimation of service loads

It was intended that the specimens be tested at loads representative of those they would experience in normal service conditions. The relationship between the expected load carrying capacity, or resistance, of a connection is defined by the statistical properties and partial factors applied by design codes.

In design according to Eurocode 5 (EN 1995), either tests or an empirical calculation based on density are used to determine a characteristic value of the embedment strength of the timber, which is exceeded by 95% of specimens. The expected value, the mean embedment strength, is higher than this characteristic value. In the tests by Santos et al. (2010), a standard deviation of 13% for the parallel-to-grain specimens and 18% for perpendicular to grain was recorded. Assuming a normal distribution, the 95th percentile will be approximately two standard deviations below the mean. Taking the average of the two grain orientations, the 95th percentile would be approximately 70% of the mean value.

The design value of a resistance R_d is then obtained from (1), in which R_k is the characteristic value of the resistance.

$$R_d = \frac{k_{mod}}{\gamma_M} \tag{1}$$

The material partial factor γ_M is taken as 1.3 for solid timber, and k_{mod} as 0.9 for a short term action. The design value is therefore 70% of the characteristic value, and therefore approximately 50% of the mean value.

Eurocode 1 (EN 1991) uses characteristic values of loads that are deemed to be exceeded once in 50 years. The relationship of the mean load to the characteristic load will vary depending on the load in question; the self-weight will vary very little during the life of a structure, while the imposed loads may vary much more. The design value of an applied load is obtained using factors in Eurocode 1, which are recommended as 1.35 for a permanent action, and 1.5 for a variable action. Applying these load factors means that, in the one in 50 year occurrence the applied load will be 30 to 35% of the mean value of the load carrying capacity.

The peak loads applied during these tests were chosen to be 20% of the predicted characteristic yield force. A detailed analysis of the variation in loads applied to a structure during its life is beyond the scope of this work, but, on the basis of the forgoing discussion, this is considered to be within the range of loads the timber might experience in service as part of a timber connection in a building or bridge structure.

3.1.3 Load time-history

The dynamic tests used a sinusoidal variation of force at a frequency of 1Hz. The relative magnitude of the oscillating force was defined by the R-ratio, which is given by the highest compressive load F_{peak} divided by the lowest compressive load F_{trough}, as shown in (2).

$$R = \frac{F_{peak}}{F_{trough}} \tag{2}$$

A nominal R-value of 1.2 was used for the tests.

The applied force time-history is shown in Fig. 3. The applied compressive force steps from zero to the minimum value of the oscillating force. The oscillating force, defined by the R-value of 1.2, is then applied for 1000 seconds. The oscillating force then ceases, and the static force is removed.

The test was repeated for each of the three different types of specimen: a 20mm dowel in Douglas Fir, a 12mm dowel in Norway Spruce and a screw in Norway spruce. For each of these combinations of timber and connector, three repetitions were carried out in each grain orientation, resulting in a total of 18 tests.
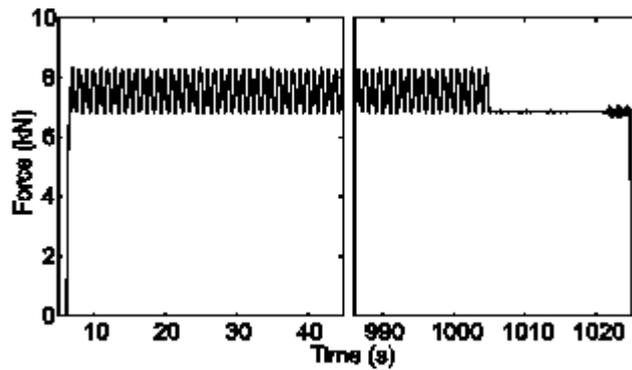
Fig. 3 Applied force

3.2   Analytical method

3.2.1   Observed behaviour

Before presentation of the model which has been used to represent the embedment behaviour, a qualitative discussion of the behaviour it represents is considered necessary.

The displacement of the dowel due to the applied force shown in Fig. 3 is illustrated in Fig. 4. First, there is a deformation that occurs simultaneously with the applied force. After the initial deformation, and during the cyclic applied force, there is evidence of a viscoelastic component which responds gradually to the step in applied force over the 1000s duration of the load. When the applied force returns to zero, there is a significant unrecovered deformation.

At this timescale, there is no clear evidence of a tendency towards a constant rate of creep. The viscoelastic creep appears to decay so that the mean displacement in each cycle tends towards a constant value. The creep that would be expected to occur under load applied for a period of hours or days is not evident in these tests.
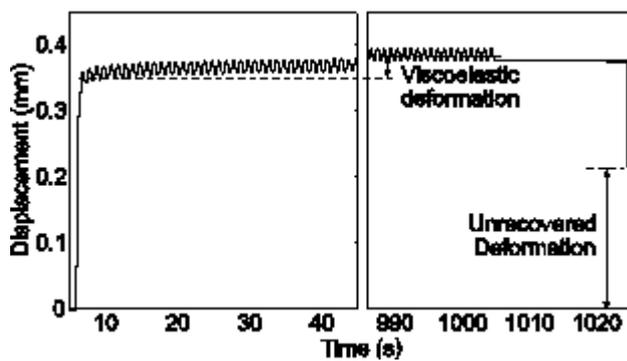

Fig. 4 Displacement under oscillating load

3.2.2   Rheological model

The basic mechanical model of a Kelvin-Voigt viscoelastic material consists of a linear elastic spring and a linear viscous damper in parallel. The response of a single Kelvin-Voigt element to a step in applied force is given by (3). X represents the elastic displacement towards which the displacement of the element tends. The time constant τ is, therefore, the time at which the displacement reaches approximately $0.63X$. A

short time constant represents near-elastic behaviour and a long time constant represents near-viscous behaviour.

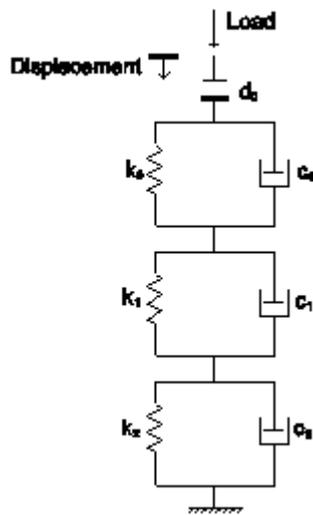$$x = X \left(1 - e^{\frac{t}{\tau}}\right) \tag{3}$$

Fig 5. Rheological model

In developing this model, the first step was to examine the near-elastic, or lightly-damped, component of the response. One near-elastic response could be measured as the secant stiffness of each cycle of oscillating load, and another as the initial response to the step in applied load at the start of the test. It was found that the initial stiffness was much lower than the secant stiffness. Since the secant stiffness was relatively constant throughout the test, it was thought that the lower initial stiffness could be explained by transient effects under first loading. This difference in stiffness was therefore represented by a gap element assumed to close under initial loading and remain closed under the oscillating load. The nature of this transient effect is further discussed in Section 4.3.

The next step was to address the viscoelastic deformation which was observed during the time under oscillating load. A single Kelvin-Voigt element was added, and fitted to match the displacements at the midpoint and the end of the test, at 500 and 1000s. The model with the gap element, near-elastic element and this viscoelastic element reproduced the steady-state stiffness under oscillating load, and followed the displacement response well in the second half of the test. In the first half of the test, the modelled displacement was much lower than the measured displacement, with the peak discrepancy at approximately 40s. A further viscoelastic element was therefore added with a shorter time-constant than the previous one, to match the faster component of the response of the real system. Since the maximum discrepancy was at approximately 40s, the additional viscoelastic element was adjusted to match the displacements at 20 and 40s.

The proposed model therefore consists of three Kelvin-Voigt elements. One, which will be referred to as the near-elastic element, has a time constant of the order of 0.01s, stiffness k_0 and damping c_0. This element represents the stiffness and energy dissipation under oscillating load. The second has a time constant of approximately 20s, referred to as the balanced element with stiffness k_1 and damping c_1, and the third has a time constant of approximately 500s, referred to as the near-viscous element with stiffness k_2 and damping c_2. The latter two elements represent the viscoelastic deformation in the duration of the tests.

Under an oscillating load at 1Hz, neither the balanced or near-viscous elements move significantly due to their relatively high damping, so the majority of the differential movement is in the near-elastic element. The near-elastic element does, however, show hysteresis at this frequency, and so models the hysteretic energy dissipation in the specimen at 1Hz.

A constant deformation of d_0 is added to the deformation in the viscoelastic model, represented by the gap element in the mechanical model. This allows for the displacement associated with the unevenness of the interface between dowel and timber and the imperfect fit of the dowel in the drilled hole. This phenomenon is discussed further in Section 4.3.

Part of the deformation represented by d_0 may be recovered upon removal of the load. The scope of this model is, therefore, only to represent the response of the connection to a step in applied load and an oscillating load. It is not intended to differentiate between the reversible and irreversible components of the deformation.

Friction between dowel and timber has been shown by Sjödin et al. (2008) to affect the distribution of strain in the timber, and so the slip between the dowel and the timber may give energy dissipation. The model of the response of the connection, therefore, represents not just the viscoelastic behaviour of the timber parent material, but the frictional interaction between the dowel and the timber. To preserve the simplicity and linearity of the model, coulomb friction elements are not included, and the frictional component of the response is therefore allowed for in the stiffness and viscous damping in the viscoelastic elements. A coulomb friction model predicts no variation of energy dissipation with frequency of loading, while a viscous damper dissipates energy in proportion to frequency. This suggests that the Kelvin-Voigt model may not predict the frequency dependence of damping accurately, but that effect is not investigated in this study.

3.2.3   Curve fitting procedure
The parameters for the model were derived by considering the response of the specimen to the step in applied load and to the oscillating load. The following process was implemented using MATLAB®.

The response of the system to a step in applied load is approximately given by (4), the near-elastic element being assumed to respond immediately, contributing to X_0.

$$x = X_0 + X_1 \left(1 - e^{\frac{-t}{\tau_1}}\right) + X_2 \left(1 - e^{\frac{-t}{\tau_2}}\right) \tag{4}$$

$X_{1,2}$ and $\tau_{1,2}$ are related to the parameters in the balanced and near-viscous component by (5) and (6).

$$X_{1,2} = \frac{1}{k_{1,2}} \tag{5}$$

$$\tau_{1,2} = \frac{c_{1,2}}{k_{1,2}} \tag{6}$$

X_0 represents both d_0 and the displacement due to the near-elastic element, as shown in (7). Since neither the balanced or near-viscous elements move significantly under the oscillating load, the stiffness k_0 can be determined as the secant stiffness in each cycle.

$$X_0 = d_0 + \frac{F}{k_0} \tag{7}$$

(4) contains 5 unknown values: X_0, X_1, X_2, τ_1 and τ_2. 4 points in the measured displacement were used to calculate these parameters for the model: at 20, 40, 500 and 1000 seconds after initial loading. The displacement d_0, which occurs in addition to the viscoelastic behaviour, was estimated and found iteratively.

The curve-fitting procedure was as follows: First, time zero was set to correspond to the midpoint of the application of the force at the start of the test. k_0 was calculated using the average secant stiffness of the specimen under the oscillating load. k_0 and an assumed deflection d_0, which would be revised later, were used to calculate X_0.

The parameters of the balanced element, X_1 and τ_1, were then defined based on the displacement X_0, and that at 20 and 40 seconds, using (4). It was assumed that the contribution of the near-viscous element at these times is small.

The deflection due to X_0 and the balanced element was then subtracted from the measured deflection. The remainder of the deflection was assumed to be due to the near-viscous element and the values at zero, 500 and 1000 seconds were used to define X_2 and τ_2. d_0 was then adjusted, and the process repeated iteratively until the appropriate value of d_0 was found, for which the modelled deflection at the initial peak in applied load matched the measured deflection.

The energy dissipated in each cycle of applied force was measured from each cycle in the force-displacement diagram as the area inside the hysteretic loop. The parameter c_0 could then be found using (8), where E_d represents the energy dissipated, f the frequency and ΔF the range of the oscillating force. In order to capture the steady-state energy dissipation, the average from the final 300 cycles was used to define the damping in the near-elastic element.

$$E_d = 2\pi^2 f c_0 \left(\frac{\Delta F}{k_0}\right)^2 \qquad (8)$$

3.2.4 Application to measured force time-history

The model was applied to the same time-history of force as applied to the specimen, using an Euler time-stepping method. The experimental measurements were taken at a sampling rate of 100Hz but, in order to ensure the stability of the Euler method, the measured force was interpolated so that the Euler method was applied to a force time history with 1000 samples per second.

4 Results and discussion

4.1 Model accuracy

The measured and modelled values of displacement are plotted against time in Fig. 6. It can be seen that the modelled response closely follows the response of the specimen, the largest error being during the first 5 to 10 cycles of load. The near-elastic element gives the correct amplitude of displacement due to the oscillating load throughout the test, and the balanced and near-viscous elements follow the creep over the 1000 second duration of the test. In a similar way that, as described in Section 3.2.2, the discrepancy between measured and modelled displacement in the first half of the test was reduced by the addition of another viscoelastic element with shorter time constant, the discrepancy in the first 5 to 10 cycles could be reduced by addition of a further viscoelastic element with an even shorter time constant. It is considered, however, that the current model, consisting of three Kelvin-Voigt elements, gives a sufficiently accurate representation for the purpose of the comparisons made between specimens in Section 4.2.
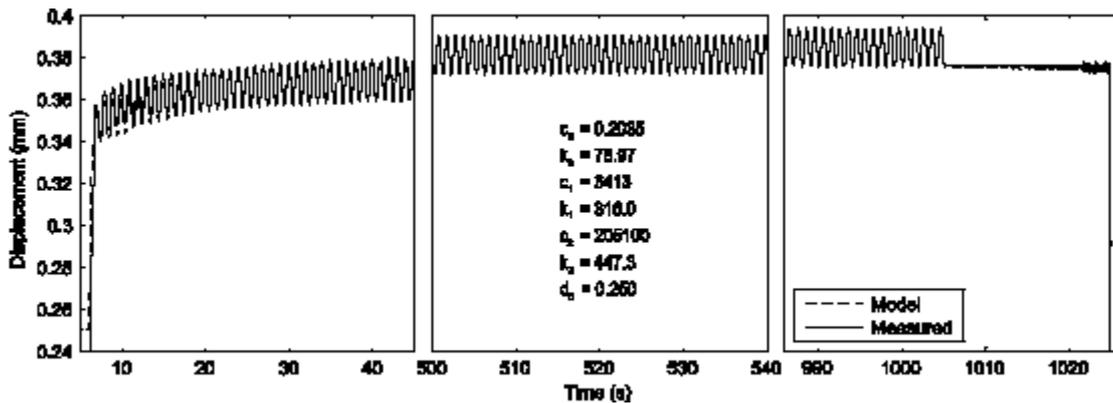

Fig. 6 Comparison of displacement time-history between measured response and rheological model

Fig. 7 shows the 15th, 500th and 1000th cycles of applied force, plotted against displacement. It is shown that the rheological model captures the creep between each cycle, shown by the movement of the cycles from left to right. Also captured is the transient contribution that creep makes to energy dissipation, shown by the higher energy dissipation in the 15th cycle. The energy dissipation is given by the area inside

the hysteretic loops, and noted as E_d in Fig. 7. The steady-state energy dissipation, represented by the damping in the near-elastic element of the rheological model, is thought to result from both a consistent hysteresis in the timber, and the friction between the dowel and the timber.
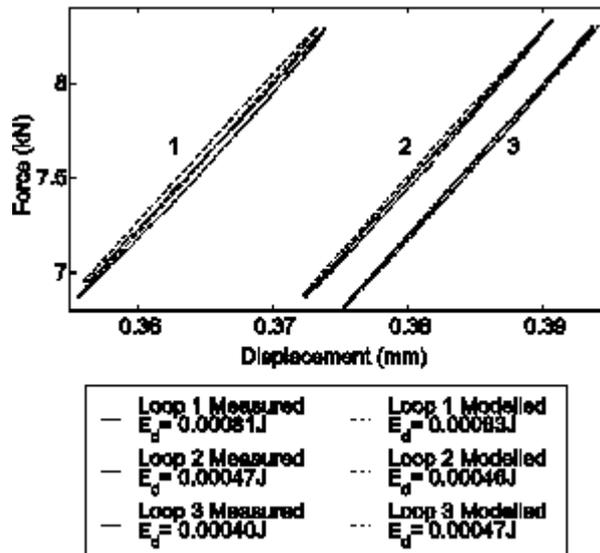

Fig. 7 The 15th, 500th and 1000th force-displacement cycles - E_d represents the energy dissipated in each cycle

One of the simplifications inherent in this model is that the procedure used to fit the model to the experimental results considers only the time under the mean load, and not the number of cycles of load applied. It is considered that this approach is suitable because of the relatively small magnitude of the oscillating component of the load compared with its mean. A good representation of the overall behaviour has been achieved by considering the viscoelastic response to the mean load, and superimposing upon that the response to the oscillating load as a separate lightly-damped element. The small amplitude and high frequency of the oscillating component means that the heavily-damped parts of the model, the balanced and near-viscous elements, do not have a significant response at the frequency of the oscillating load, and can be considered as responding to a constant load at the mean value.

The fact that the heavily-damped parts of the model are derived based only on the mean of the oscillating load doesn't mean they don't affect the oscillating response, however, and it is shown, in Fig. 6 and Fig. 7, that the model reflects the measured transient effects on displacement and damping. It is noted that this approach may not be suitable for larger amplitudes of oscillating load, but it is considered that this model, and the approach used to fit it to the experimental results, captures several important features of the behaviour of timber in embedment due to the small-amplitude vibration which is regularly experienced by structures in service.

4.2   Comparison of specimens

For each specimen, three equivalent stiffnesses are presented, based on the parameters of the fitted rheological model. They are illustrated in Fig. 8. The first, which will be referred to as the dynamic stiffness k_d, is equal to k_0, the stiffness of the near-elastic element. This is the stiffness which would determine the natural frequency of a

structure containing this type of connection, oscillating in the range used in these tests.
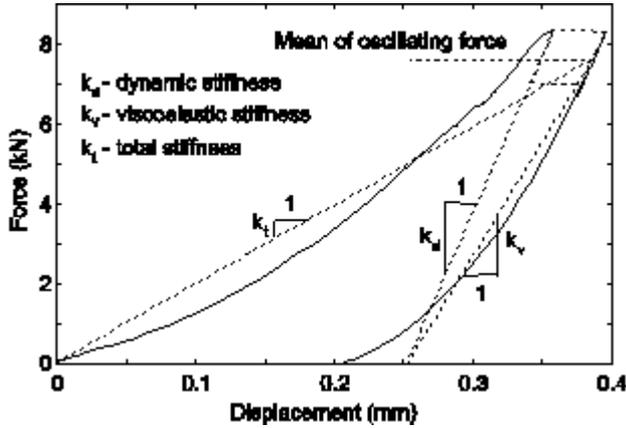

Fig. 8 The three equivalent stiffnesses used to describe the response of each specimen - the 1000 cycles at 1Hz have been omitted for clarity

The second equivalent stiffness is the series combination of k_0, k_1 and k_2, as in (9), and represents the stiffness under a static load, once all the viscoelastic elements have relaxed. This is called the viscoelastic stiffness k_v. It only includes the viscoelastic components which are apparent over the 1000 second duration of these tests, so it represents the stiffness appropriate to calculate the relative displacement due to a short-term static load, such as crowd, wind or vehicle loading on a structure.

$$k_v = \left(\frac{1}{k_0} + \frac{1}{k_1} + \frac{1}{k_2} \right)^{-1} \tag{9}$$

The third equivalent stiffness is called the total stiffness k_t, and includes the viscoelastic stiffness combined with the effect of d_0. This stiffness would be appropriate to calculate the total deformation of the connection from initial loading due to, for example, the self-weight and imposed loads on a structure. It does not allow for longer-term creep effects which were not apparent in the 1000 second test. The total equivalent stiffness is given by (10).

$$k_t = \left(\frac{1}{k_v} + \frac{d_0}{F_{av}} \right)^{-1} \tag{10}$$

Fig. 9 shows the equivalent stiffnesses plotted for each specimen tested. The three equivalent stiffnesses are substantially different in each specimen. For example, over the complete set of tests the dynamic stiffness is, on average, 3.8 times higher than the total stiffness. This difference suggests that each type of behaviour would be best represented in elastic analysis by a different value of stiffness, and shows the importance of consideration of the nature of the loading in determining an equivalent stiffness for a connection.
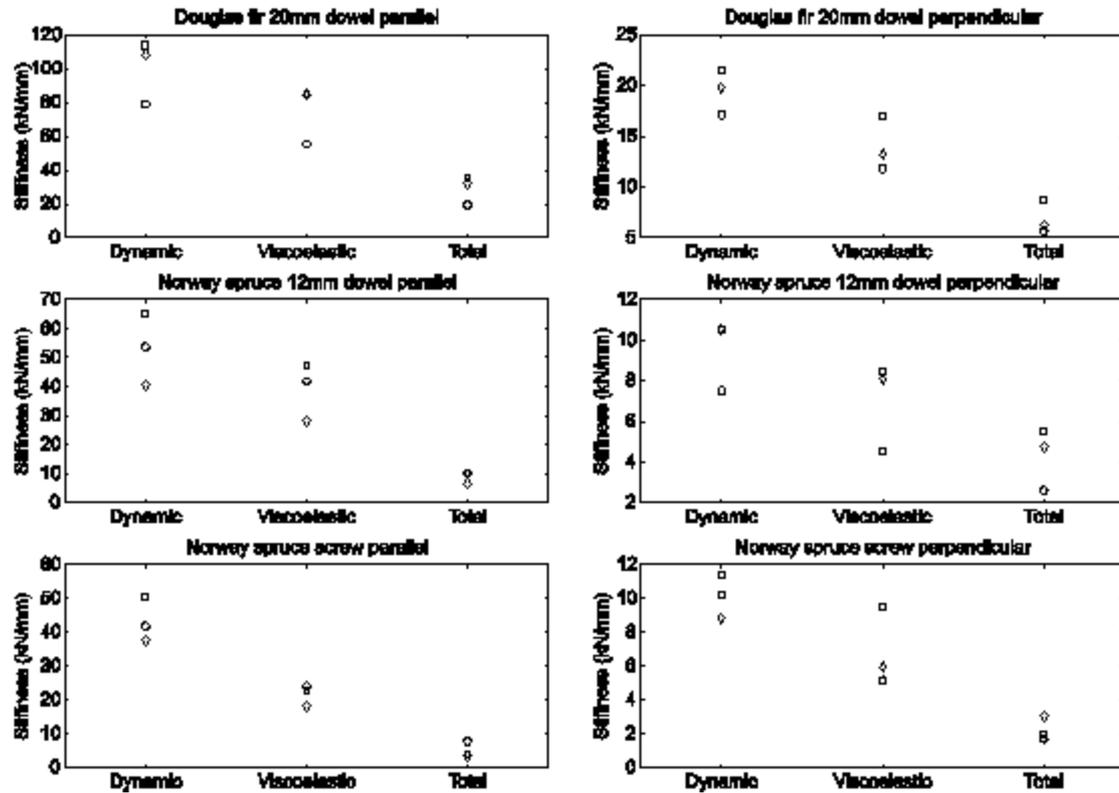
Fig. 9 Equivalent stiffness calculated using fitted rheological model parameters

Table 2 shows the mean of the stiffness for each of the three repetitions of each type of specimen and orientation. The stiffness is also expressed as the foundation modulus K, given by (11), where w is the length of the specimen along the dowel axis, and d is the dowel diameter.

$$K = \frac{k}{wd} \tag{11}$$

The ratio of the viscoelastic stiffness to the dynamic stiffness is consistent between the dowel specimens. This suggests that it may be possible to develop an empirical relationship between these equivalent static stiffnesses, on the basis of further tests, which could be used in design.

The total stiffness depends on the contribution from d_0, which is thought to depend on errors in construction such as oversize of the hole due to movement of the drill bit, and on the quality of the interface between dowel or screw and timber. These parameters are difficult to control, and can be expected to vary between individual specimens. The variation in total stiffness was, therefore, expected.

Table 2 Mean stiffness and foundation modulus from rheological model

Specimen	Orientation	Mean dynamic stiffness k_d kN/mm	Mean dynamic foundation modulus K_d kN/mm^2/ mm	Visco-elastic k_v or K_v %	Total k_t or K_t %
Douglas fir and 20mm dowel	Parallel	100.30	83.58	75%	29%
	Perpendicular	19.48	16.23	72%	35%
Norway spruce and 12mm dowel	Parallel	53.13	110.68	74%	17%
	Perpendicular	9.53	19.85	74%	45%
Norway spruce and screw	Parallel	43.30	144.33	50%	12%
	Perpendicular	10.15	33.84	68%	22%

4.3   Initial plastic deformation

Some further discussion of the nature of the displacement d_0 is considered appropriate, since it represents a large proportion of the total deformation of the connection, and appears to be far from linear-elastic.

If the dowel and the half-hole in the timber member do not have exactly the same diameter, then the dowel will initially make contact with the timber along a single line along its length. Any unevenness in the surface of the timber will mean that the line is split into a series of shorter lines or points. As a force is applied to the dowel, the pressure on this, initially very small, bearing area will be very high. It appears that this initial high pressure is sufficient to cause deformation of the timber in small volumes around the dowel, enough that the force is spread over a larger area and the pressure reduced.

The result is that a significant part of the initial deformation of the dowel under first loading is made up of the deformation which accommodates these stress concentrations, which may be plastic in parts of the timber, and elastic in others. Under subsequent dynamic loading, especially when the force remains above the level at which all these imperfections are crushed, the imperfections have little effect on the stiffness of the specimen. It is believed that this behaviour results in the deflection d_0 in the model, which was incorporated so that the viscoelastic model could be fitted to the rest of the response.

On the basis of this explanation, the deformation d_0 would be expected to depend on the magnitude of the applied force, but would be expected to tend toward some value, at which all of the imperfections in the contact surface were taken up.

4.3.1   Microscopy

In order to test the hypothesis that stress concentrations produce plastic deformation in small volumes of the timber around the dowel, optical microscopy has been used to observe the microstructural changes between specimens before and after loading. The plane in which each specimen was cut is shown in Fig. 10. With the specimens cut in these planes, the microscope view is along the axis of the tracheids for the perpendicular-to-grain specimen and along the dowel axis for the parallel-to-grain specimen.
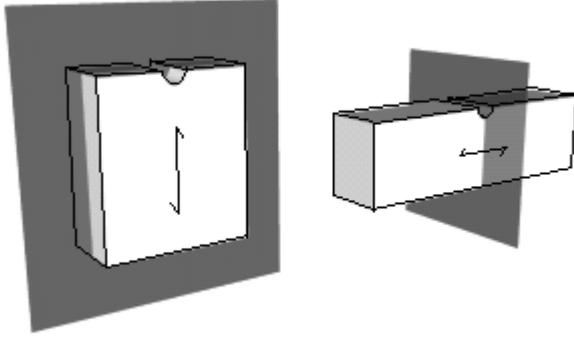
Fig. 10 Cutting planes for microscopy

The specimens for microscopy were prepared by cutting followed by sanding with P600 silicon carbide paper. The surface was then cleared of dust with an air jet. In the case of the perpendicular-to-grain specimen, the air jet did not remove the particles which had filled the pores, and so a plane surface was created by the cell walls and the dust filling each pore.

a and **c** in Fig. 11 show the microstructure in each orientation for specimens which had remained unloaded. In the perpendicular-to-grain specimen, the cells appear to have been undamaged in this plane by drilling and cutting. In the parallel-to-grain specimens, the tracheids at the edge of the hole curve slightly. This is thought to be a consequence of either drilling during manufacture, or cutting or sanding during preparation for microscopy. The fact that all tracheids were observed to curve tangentially suggests that drilling is the most likely cause.
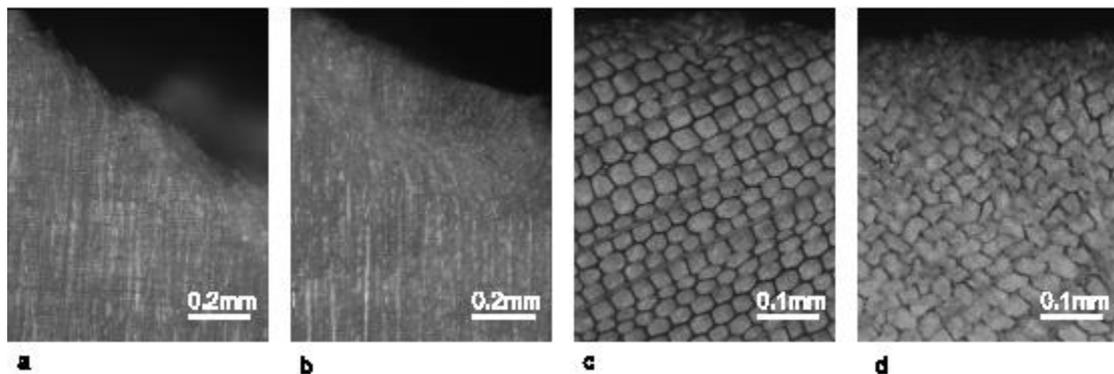

Fig. 11 Microscope images showing: **a** parallel-to-grain specimen which has not been loaded by a dowel; **b** parallel-to-grain specimen loaded to a peak load of 40% of its predicted yield load; **c** perpendicular-to-grain specimen which has not been loaded; **d** perpendicular-to-grain specimen loaded to a peak load of 40% of its predicted yield load

A similar image for a perpendicular-to-grain specimen which has seen an applied force 40% of its predicted yield force is shown in **d** in Fig. 11. In this specimen, the tracheids near the edge of the hole can be seen to have been permanently crushed.

The process of these tracheids being crushed forms part of the irreversible deformation which occurs under initial loading. There are also some areas of intact tracheids around the edge of the hole, which suggests that the crushing of the

tracheids acts to allow force to be distributed to these areas, which may initially have been recessed. It is thought that the crushing process, therefore, spreads the applied force over a larger contact area, increasing the stiffness of the connection.

In the parallel-to-grain specimen, the force is not applied in the direction which would cause crushing of the tracheids. A similar process of initial irreversible deformation followed by viscoelastic behaviour occurs, however, and the microscope image in **b** in Fig. 11 shows a possible cause of that initial deformation. In the specimen, loaded to 40% of its predicted yield force, some buckling of the tracheids can be seen, away from the edge of the hole. This buckling is distinct from the curvature of the tracheids which was observed in the unloaded specimen, in that it does not occur immediately at the edge of the hole. As with the perpendicular-to-grain specimen, some undamaged areas were also visible, suggesting that the irreversible deformation acts to take up unevenness in the contact face between the dowel and the timber.

The magnitude of the initial plastic deformation varies widely between the specimens tested, which is consistent with the hypothesis that it is caused by unevenness in the contact surface between the dowel and the timber and lack of fit between the dowel and the hole. Both of these parameters depend on the accuracy of the manufacturing process.

5   Conclusion

A simple model has been proposed and tested to represent the response of a block of timber under dynamic dowel-bearing. It has been shown that the model replicates the viscoelastic response of the specimens which have been tested, capturing the response to the step in applied load, the creep under the mean applied load and the secant stiffness under oscillating load. The energy dissipation under each cycle of applied load is modelled, along with the transient contribution made by creep to this energy dissipation.

In order for this linear viscoelastic model to be successfully applied, an allowance was made for the initial plastic deformation in the timber around the dowel. Microscope analysis of specimens before and after testing showed the nature of this plastic behaviour to be crushing of trachieds under perpendicular-to-grain load, and buckling of fibres under parallel-to-grain load.

The application of this model highlights several aspects of the behaviour of timber in dowel-bearing under oscillating load. One is that the initial deformation due to lack of fit between the dowel and the hole and unevenness in the contact surface represents a large proportion of the total deformation under its first loading. This deformation adds to the viscoelastic deformations to give the total deformation under the mean load. In a structure this will represent the total static deformation of the connection, which should be used for consideration of serviceability requirements such as the visual acceptability of deflections and the compatibility of deflections with cladding and furnishing elements.

Under oscillating load, however, the secant stiffness of the specimen is defined almost entirely by the short time constant component of the model. This leads to a higher

equivalent stiffness of a structural connection, which should be used to calculate the natural frequency of the structure for vibration serviceability.

In order to use these equivalent stiffnesses to calculate the deformation of a real structural connection, a model which incorporates the deformation of the dowel would be required. That model is outside the scope of this work, but has been widely studied, as described in Section 2.

The model has shown the different components of the dowel-bearing behaviour of timber, and highlights the different requirements for stiffness evaluation of dowel-type timber connections depending on the nature of the applied load. Where structures are modelled with semi-rigid connections to allow for this stiffness, they should use either a non-linear stiffness, or an equivalent linear stiffness appropriate to the nature of the applied load.

The model parameters derived here are likely to apply only to the frequency of oscillation, R-ratio and peak force tested in this study. In particular, it is not anticipated that the viscous elements will accurately predict the variation of energy dissipation with frequency, and, under larger-amplitude oscillation, the assumption that the response of the balanced and near-viscous elements can be derived using the mean value of the oscillating force may not be valid. There is potential for future work to investigate and model the frequency dependence of embedment stiffness and energy dissipation, and the response to larger-amplitude oscillating loads. This model does, however, provide a tool for identifying and understanding the different components of the embedment response of a connector in timber under small-amplitude oscillating load, which is a form of loading commonly imposed on structures by, for example, wind or footfall.

References

ASTM D 5764:1997 Standard Test Method for Evaluating Dowel-Bearing Strength of Wood and Wood-based Products (Reapproved 2002). Volume 4.10. ASTM, West Conshohocken, PA

Awaludin A, Hayashikawa T, Hirai T, Oikawa (2007) A Dynamic Response of Moment Resisting Timber Joints. Paper presented at the 8th Pacific Conference on Earthquake Engineering, Singapore, pp 5-7

Awaludin A, Hirai T, Hayashikawa T, Sasaki Y, Oikawa A (2008a) Effects of pretension in bolts on hysteretic responses of moment-carrying timber joints. J Wood Sci 54 (2):114-120.

Awaludin A, Hirai T, Hayashikawa T, Sasaki Y, Oikawa A (2008) One-year stress relaxation of timber joints assembled with pretensioned bolts. J Wood Sci 54 (6):456-463.

Burgers JM (1939) Mechanical considerations - Model systems - Phenomenological theories of relaxation and of viscosity. In: First Report on Viscosity and Plasticity. 2nd edn. N.V. Noord-Hollandsche Uitgevers Maatschappij, Amsterdam, pp 27-30

Chui Y, Li Y (2005) Modeling Timber Moment Connection under Reversed Cyclic Loading. Journal of structural engineering 131 (11):1757-1763.

Chui Y, Ni C (1997) Load-Embedment Response of Timber to Reversed Cyclic Load. Wood Fiber Sci 29 (2):148-160

Dinwoodie JM (2000) Timber its nature and behaviour. 2nd ed. edn. Spon, London

Ehlbeck J, Larsen HJ (1993) Eurocode 5-Design of timber structures: Joints. In: International workshop on wood connectors, Madison, USA, 1991. Forest Products Society, pp 9-23

EN 383:2007 Timber structures. Test methods. Determination of embedment strength and foundation values for dowel type fasteners. BSI.

EN 1991-1-4:2005 Eurocode 1 Actions on Structures. Part 1-4 General Actions - Wind Actions. BSI.

EN 1995-1-1:2004+A1:2008 Eurocode 5 Design of timber structures. Part 1-1: General — Common rules and rules for buildings,. BSI.

Foschi RO (2000) Modeling the hysteretic response of mechanical connections for wood structures. Paper presented at the World Conference of Timber Engineering, Whistler, B.C., Canada.

Foschi RO, Yao F, Rogerson D (2000) Determining Embedment Response Parameters from Connector Tests. Paper presented at the World Conference on Timber engineering, Whistler, B.C., Canada.

Gressel P (1984) Zur Vorhersage des langfristigen Formänderungsverhaltens aus Kurz-Kriechversuchen. Holz als Roh- Werkst 42 (8):293-301.

Hering S, Niemz P (2012) Moisture-dependent, viscoelastic creep of European beech wood in longitudinal direction. Eur J Wood Prod:1-4.

Jiali J, Jianxiong L (2009) Anisotropic characteristics of wood dynamic viscoelastic properties. For Prod J 59 (7/8):59-64

Lagana R (2008) Creep parameters of spruce wood in high temperature environment. Madera Cienc Tecnol 10 (1):19

Santos CL, De Jesus AMP, Morais JJL, Lousada JLPC (2010) A Comparison Between the EN 383 and ASTM D5764 Test Methods for Dowel-Bearing Strength Assessment of Wood: Experimental and Numerical Investigations. Strain 46 (2):159-174.

Schniewind AP, Barrett JD (1972) Wood as a linear orthotropic viscoelastic material. Wood Sci Technol 6 (1):43-57.

Sjödin J, Serrano E, Enquist B (2008) An experimental and numerical study of the effect of friction in single dowel joints. Eur J Wood Prod 66 (5):363-372.

Sun N, Das S, Frazier CE (2007) Dynamic mechanical analysis of dry wood: Linear viscoelastic response region and effects of minor moisture changes. Holzforsch 61 (1):28-33.